Spectrochimica Acta, Vol. 40A, No. 6, pp. 503–517, 1984
Printed in Great Britain.

0584–8539/84 $3.00 + 0.00

Vibrational analysis of crystalline diketopiperazine—II. Normal mode calculations*

T. C. CHEAM and S. KRIMM
Department of Physics and Biophysics Research Division, University of Michigan, Ann Arbor, MI 48109, U.S.A.

(*Received* 29 *November* 1983)

Abstract—Based on our Raman and i.r. [1] data and assignments for DKP and five of its isotopic derivatives, we have refined an intramolecular force field in a non-redundant basis. This analysis shows that the *cis* peptide group may be best differentiated from the *trans* by the presence of an NH out-of-plane bend mode in the 800 cm^{-1} region. Several atom–atom potentials have been evaluated for their ability to explain observed lattice frequencies and internal mode splittings. Observed splittings in CO stretch modes can be accounted for by dynamical charge transfer and transition dipole coupling interactions.

INTRODUCTION

In this paper we describe the refinement of an intramolecular force field for diketopiperazine (DKP) and five isotopic derivatives, using the Raman and i.r. data and assignments presented in the previous paper [1]. Our aim is to check our empirical assignments and to understand the vibrational modes of DKP in more detail. We also hope to use the DKP force field as a basis for analysing other molecules with *cis* peptide groups.

The derivation of a valence force field for a molecule like DKP is complicated by the numerous cyclic and branching redundancies. The force constant matrix in redundant coordinates is not unique: different sets of force constants can reproduce the same set of frequencies [2]. The result is that such force constants are correlated with each other and cannot be refined together [3, 4]. This fundamental correlation among force constants in a redundant basis should be distinguished from the accidental correlation that can arise in any basis because of insufficient data. The first type of correlation can be removed by transforming to a non-redundant basis. The second type can be reduced by adding more data or by transforming to a basis closer to the normal coordinates, so that the number and magnitude of the off-diagonal elements needed are reduced. It is advantageous to choose a basis that facilitates the refinement of a force field; at the end, one may transform the force constants to any other basis. In our calculations, we have made several transformations of the internal coordinates with the aim of coming up with well-determined force field parameters and, therefore, more reliable descriptions of the normal modes.

Because the data used in the refinement are on crystalline samples, we have taken into account intermolecular interactions in the calculation. In lattice dynamical calculations of hydrocarbons it is now common to include intermolecular interactions of the atom–atom type. Several sets of empirical potential parameters have been derived for hydrocarbon crystals, using static and dynamical data [5]. By contrast, few vibrational analyses of peptides consider a full set of intermolecular interactions. Previous calculations from our laboratory on crystalline polypeptides [6] have emphasized the importance of transition dipole coupling interactions in explaining factor group splittings of modes that have strong i.r. intensity, such as amide I. Other intermolecular interactions were ignored except for the NH . . . OC hydrogen bond and nearest neighbor H . . . H contacts.

We will give the results of calculations using the atom–atom potentials of HAGLER *et al.* [7, 8] and of MOMANY *et al.* [9]. These potentials were derived using static properties of amide crystals, and were shown [7, 8, 10] to give minimum-energy structures of DKP that are in good agreement with the X-ray structure [11]. Although these potentials have been applied in conformational studies on peptides and polypeptides [12, 13], to our knowledge their performance in lattice dynamical calculations has not been examined.

NORMAL MODE CALCULATIONS

The crystal structure of DEGEILH and MARSH [11] was used. The apparent CH and NH bond lengths (CH = 0.93, 0.95 Å; NH = 0.86 Å) obtained in this X-ray study are significantly shorter than values commonly observed by neutron diffraction and spectroscopic techniques. The primary causes of the discrepancies are bonding effects, thermal motion and the weak scattering of X-rays by hydrogen atoms [14]. We therefore "stretched out" the CH bonds to 1.09 Å and the NH bond to 1.00 Å; the angles involving the H atoms are probably more reliable and were not modified.

We used in our calculation the method of KOBAYASHI [15], in which the secular equation is set up in a Cartesian coordinate basis and factored using

*This is paper number 23 in a series, "Vibrational analysis of peptides, polypeptides and proteins", of which [1] is paper number 22.

the symmetry operations of the factor group. In DKP the factor group is isomorphic to C_{2h}, and four symmetry blocks result: A_g, B_g, A_u and B_u, each of dimension 21×21. In deriving the intermolecular Cartesian coordinate force constants from the atom–atom potentials, we did not include the so-called "linear term"; this is because we did not perform an energy minimization of the DKP crystal [16].

The primitive internal coordinates R for one asymmetric unit are listed in Table 1 with the numbering of atoms shown in Fig. 1. The out-of-plane angle bends

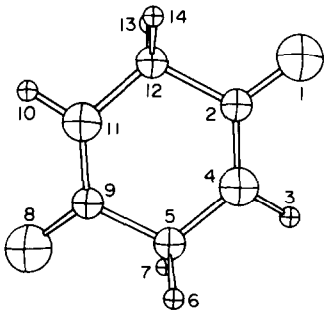

Fig. 1. Diketopiperazine molecule atom numbering.

Table 1. Primitive internal coordinates

Coordinate	Atoms
$R_1 = \Delta r(CO)$	1,2
$R_2 = \Delta r(NH)$	3,4
$R_3 = \Delta r(CH)$	5,6
$R_4 = \Delta r(CH)$	5,7
$R_5 = \Delta r(CN)$	2,4
$R_6 = \Delta r(NC^{\alpha})$	4,5
$R_7 = \Delta r(C^{\alpha}C)$	5,9
$R_8 = \Delta\theta(C^{\alpha}CN)$	12,2,4
$R_9 = \Delta\theta(C^{\alpha}CO)$	12,2,1
$R_{10} = \Delta\theta(NCO)$	4,2,1
$R_{11} = \Delta\theta(CNC^{\alpha})$	2,4,5
$R_{12} = \Delta\theta(CNH)$	2,4,3
$R_{13} = \Delta\theta(C^{\alpha}NH)$	5,4,3
$R_{14} = \Delta\theta(NC^{\alpha}C)$	4,5,9
$R_{15} = \Delta\theta(NH^{\alpha}H)$	4,5,6
$R_{16} = \Delta\theta(NC^{\alpha}H)$	4,5,7
$R_{17} = \Delta\theta(CC^{\alpha}H)$	9,5,6
$R_{18} = \Delta\theta(CC^{\alpha}H)$	9,5,7
$R_{19} = \Delta\theta(HC^{\alpha}H)$	6,5,7
$R_{20} = \Delta\omega(CO)$	2,1,12,4
$R_{21} = \Delta\omega(NH)$	4,3,2,5
$R_{22} = \Delta\tau(CN)$	2,4
$R_{23} = \Delta\tau(NC^{\alpha})$	4,5
$R_{24} = \Delta\tau(C^{\alpha}C)$	5,9

$\Delta\omega$ and torsions $\Delta\tau$ are defined as in [17]. Because of the low molecular symmetry, the redundancy relations among the R_is are rather complicated and are best obtained numerically. To keep the resulting non-redundant coordinates sufficiently simple, we proceeded as follows. Local symmetry internal coordinates s were formed (Table 2) to remove the six branching redundancies about the C^{α}, C and N atoms. (The redundancy relations s_{22}, s_{23} and s_{24} are not exact: the angles about the C^{α} atom are not tetrahedral, and the limited precision of the experimental atomic positions lead to planarity of the groups $C^{\alpha}CON$ and $CNHC^{\alpha}$ to no better than the third decimal place.) Next, we defined the C_i group symmetry internal coordinates S for a molecule as:

$$S_i(a_g) = \begin{cases} 1/\sqrt{2}\,(s_i + s_i') \text{ for } i = 1\text{–}16,\ 22\text{–}24 \\ 1/\sqrt{2}\,(s_i - s_i') \text{ for } i = 17\text{–}21 \end{cases}$$

$$S_i(a_u) = \begin{cases} 1/\sqrt{2}\,(s_i - s_i') \text{ for } i = 1\text{–}16,\ 22\text{–}24 \\ 1/\sqrt{2}\,(s_i + s_i') \text{ for } i = 17\text{–}21 \end{cases}$$

where s_i' is the ith local symmetry coordinate for the

Table 2. Local symmetry internal coordinates

CO str	$s_1 = R_1$
NH str	$s_2 = R_2$
CH_2 asy str	$s_3 = (R_3 - R_4)/2^{1/2}$
CH_2 sym str	$s_4 = (R_3 + R_4)/2^{1/2}$
CN str	$s_5 = R_5$
NC^{α} str	$s_6 = R_6$
$C^{\alpha}C$ str	$s_7 = R_7$
CNC^{α} def	$s_8 = (2R_{11} - R_{12} - R_{13})/6^{1/2}$
$NC^{\alpha}C$ def	$s_9 = (5R_{14} - R_{15} - R_{16} - R_{17} - R_{18} - R_{19})/30^{1/2}$
$C^{\alpha}CN$ def	$s_{10} = (2R_8 - R_9 - R_{10})/6^{1/2}$
CO ib	$s_{11} = (R_9 - R_{10})/2^{1/2}$
NH ib	$s_{12} = (R_{12} - R_{13})/2^{1/2}$
CH_2 bend	$s_{13} = (4R_{19} - R_{15} - R_{16} - R_{17} - R_{18})/20^{1/2}$
CH_2 wag	$s_{14} = (R_{15} + R_{16} - R_{17} - R_{18})/2$
CH_2 twist	$s_{15} = (R_{15} - R_{16} - R_{17} + R_{18})/2$
CH_2 rock	$s_{16} = (R_{15} - R_{16} + R_{17} - R_{18})/2$
CO ob	$s_{17} = R_{20}$
NH ob	$s_{18} = R_{21}$
CN tor	$s_{19} = R_{22}$
NC^{α} tor	$s_{20} = R_{23}$
$C^{\alpha}C$ tor	$s_{21} = R_{24}$
C redund	$s_{22} = (R_8 + R_9 + R_{10})/3^{1/2}$
N redund	$s_{23} = (R_{11} + R_{12} + R_{13})/3^{1/2}$
C^{α} redund	$s_{24} = (R_{14} + R_{15} + + R_{16} + R_{17} + R_{18} + R_{19})/6^{1/2}$

second asymmetric unit. The $B\tilde{B}$ matrix was set up in terms of S and diagonalized to obtain the linear redundancy relations for each of the two symmetry blocks [18]. Finally, we constructed, via the Schmidt process, the non-redundant coordinates in Table 3. It can be seen that, except for the coordinates called Ring str, def and tor, whose forms arise from the cyclic redundancies, our coordinates are essentially a local symmetry set. (We have rounded off the coefficients to two decimal figures to emphasize this fact; the full coefficients, as well as further details of our calculations, are given in [19].)

The poly(glycine I) force field of MOORE and KRIMM [20] was used to derive an initial set of intramolecular force constants. (A more recent PGI force field [21] was not yet completed when we started our work.) After transforming the PGI force field to our basis, we set most of the interaction terms to zero, since we wished to keep the number of parameters in our force field to a minimum. Thus, our initial intramolecular force field was essentially a diagonal one. Before proceeding with the refinement, we had to assume an appropriate intermolecular force field. We tested several sets of atom–atom potentials, comparing the calculated lattice modes (in particular, the Raman active vibrations) with our observed values. We concluded that the potentials of MOMANY *et al.* [10] gave the best results. (We will present these results later.) As MOMANY *et al.* noted, their potential for the H . . . O interaction in the NH . . . OC hydrogen bond gave force constants that are probably too large; in DKP this value would be 0.364 mdyne/Å. We found that this interaction has the largest effect on the NH str mode, and is consequently not well determined by our data. We therefore fixed the H . . . O force constant at 0.150 mdyne/Å, a more reasonable value for a medium strength hydrogen bond.

The data used in the refinement of the intramolecular force field were those presented in paper 1 [1]. Because the *A-B* splittings are all small, we refined the force field in the A_g and A_u blocks. For the CO str modes it was found that none of the atom–atom potentials gave an *A-B* splitting larger than 1 or 2 cm^{-1}. This suggested that additional interactions such as transition multipole terms would be necessary to account for the prominent splittings observed. We therefore used the average frequency of each *A-B* pair in our fitting. Several bands whose assignments or

Table 3. Non-redundant internal coordinates

g Species	
CO str	$= 1.00S_1$
NH str	$= 1.00S_2$
CH_2 as	$= 1.00S_3$
CH_2 ss	$= 1.00S_4$
Ring str1	$= 0.71(S_5 + S_7)$
Ring str2	$= 0.71(S_5 - S_7)$
NC^{α} str	$= 1.00S_6$
Ring def1	$= 0.83S_8 - 0.41S_9 - 0.37S_{10} + 0.01(-S_{13} + S_{14} - S_{16} - S_{20} + S_{21})$
Ring def2	$= 0.74S_{10} + 0.67S_9 + 0.02S_{17} + 0.01(-S_{13} + S_{14} - S_{16} + S_{19} + S_{20} + S_{21} - S_{24})$
CO ib	$= 1.00S_{11}$
NH ib	$= 1.00S_{12}$
CH_2 bend	$= 1.00S_{13} + 0.02S_{24} - 0.01S_{10}$
CH_2 wag	$= 1.00S_{14} - 0.04S_{24} + 0.02S_{10}$
CH_2 twist	$= 0.98S_{15} + 0.13S_{21} + 0.12S_{20} + 0.09S_{17} + 0.08S_{18} + 0.01(S_{10} - S_{24})$
CH_2 rock	$= 0.88S_{16} - 0.35S_{19} + 0.19(-S_{20} + S_{21}) + 0.13S_{18} - 0.11S_{17} + 0.01(-S_{10} + S_{24})$
CO ob	$= 0.88S_{17} - 0.38S_{20} - 0.21S_{19} - 0.17S_{21} - 0.09S_{18} + 0.01(S_{10} - S_{22})$
NH ob	$= 0.88S_{18} - 0.40S_{21} + 0.20S_{19} - 0.16S_{20} - 0.01S_{10}$
Ring tor	$= 0.60S_{19} - 0.59S_{20} + 0.54S_{21} + 0.01S_{10}$
u Species	
CO str	$= 1.00S_1$
NH str	$= 1.00S_2$
CH_2 as	$= 1.00S_3$
CH_2 ss	$= 1.00S_4$
Ring str1	$= 0.65(S_5 + S_7) - 0.24S_9 - 0.21S_6 - 0.19S_8 - 0.01S_{20}$
Ring str2	$= 0.54(S_5 - S_7) - 0.51S_{10} - 0.28S_8 + 0.26S_9 - 0.05S_6 + 0.01(S_{17} + S_{19})$
NC^{α} str	$= 0.83S_6 - 0.40S_9 - 0.39S_8 - 0.07S_{10} + 0.01(S_{14} - S_{20})$
Ring def	$= 0.63S_8 - 0.60S_{10} - 0.50S_9 + 0.01(-S_{13} + S_{14} + S_{15} + S_{17} - S_{18} - S_{20} - S_{21} + S_{24})$
CO ib	$= 1.00S_{11}$
NH ib	$= 1.00S_{12}$
CH_2 bend	$= 1.00S_{13} + 0.03S_{24} - 0.01S_9$
CH_2 wag	$= 1.00S_{14} - 0.04S_{24} + 0.02S_9$
CH_2 twist	$= 0.98S_{15} + 0.12(S_{19} + S_{20} + S_{21}) - 0.01(S_{18} + S_{24})$
CH_2 rock	$= 1.00S_{16} + 0.01(-S_9 + S_{24})$
CO ob	$= 1.00S_{17} + 0.01(S_{10} - S_{19} - S_{20} - S_{21} - S_{22})$
NH ob	$= 1.00S_{18} + 0.03(S_{19} + S_{20} + S_{21}) - 0.01(S_9 + S_{10})$
Ring tor1	$= 0.82S_{20} - 0.40(S_{19} + S_{21}) - 0.01S_9$
Ring tor2	$= 0.71(S_{19} - S_{21}) + 0.01S_{10}$

values are uncertain were not used. This included the i.r. CO str, CD_2 rock and ring ib modes in the C-deuterated molecules. The CH_2 str force constants in the g and u blocks were fitted only to the 2952 and 2922 cm^{-1} i.r. bands of NdDKP, and the NH str force constant was adjusted to fit the Raman ND str mode at 2290 cm^{-1}. All assigned modes were weighted by unity, except for the ^{13}C shifts which were given weights of 5.0. A few force constants were not refined from their initial values because we felt there was insufficient data to determine them reliably. The A_g ring torsional mode was very sensitive to the intermolecular potential; we decided to refine the diagonal force constant (f_{18}) to the 214 cm^{-1} Raman band of DKP in H_2O solution.

Two sets of force constants, I and II, were derived. We first refined the force field to give an acceptable fit to data on all six isotopic species. Then we adjusted a few force constants to reproduce the observed frequencies of DKP more closely.

RESULTS AND DISCUSSION

Our final sets of intramolecular force constants are given in Table 4, and the normal modes obtained with these parameters are listed in Tables 5–7. The calculated frequencies shown in the tables are for the A_g and A_u species; the A-B splittings are given beside the A frequencies. When both components of an A-B pair were observed, the observed frequency listed is the A component.

In this section we will first discuss our force field. Next, we will discuss the calculated intramolecular modes. The lattice modes and the performance of a few

Table 4. Force constants for diketopiperazine*

No.	Coordinates	Set I	Set II
	g Species		
1	CO str	7.619 (0.271)	7.313 (0.021)
2	NH str	5.211 (0.031)	5.211
3	CH_2 asy str	4.571 (0.069)	4.571
4	CH_2 sym str	4.707 (0.072)	4.707
5	Ring str1	6.408 (0.158)	6.410 (0.009)
6	Ring str2	4.654 (0.134)	4.654
7	NC^{α} str	4.922 (0.161)	4.720 (0.008)
8	Ring def1	0.526 (0.015)	0.526
9	Ring def2	1.099	1.099
10	CO ib	1.526 (0.067)	1.473 (0.003)
11	NH ib	0.557 (0.010)	0.557
12	CH_2 bend	0.512 (0.006)	0.514 (0.001)
13	CH_2 wag	0.627 (0.011)	0.681 (0.001)
14	CH_2 twist	0.647 (0.005)	0.621 (0.000)
15	CH_2 rock	0.575 (0.021)	0.563 (0.001)
16	CO ob	0.463 (0.034)	0.463 (0.001)
17	NH ob	0.321 (0.006)	0.333 (0.000)
18	Ring tor	0.093	0.093 (0.014)
19	CO str,ring str1	0.707	0.707
20	CO str,ring def2	0.273	0.273
21	CO str,NH ib	−0.095 (0.032)	−0.095
22	Ring str2,NH ib	0.095 (0.036)	0.095
23	NC^{α} str,NH ib	−0.172 (0.030)	−0.172
24	NC^{α} str,CH_2 wag	0.346 (0.029)	0.346
25	Ring def1,ring def2	0.138 (0.040)	0.138
26	NH ib,CH_2 bend	−0.026 (0.009)	−0.015 (0.000)
27	NH ib,CH_2 wag	−0.028 (0.011)	−0.028
28	CH_2 bend,CH_2 wag	0.039 (0.010)	0.039
29	CH_2 rock,CO ob	−0.138 (0.028)	−0.138
30	CH_2 rock,NH ob	−0.028 (0.036)	−0.028
31	CO ob,NH ob	0.120 (0.037)	0.120
	u Species		
1	CO str	9.125 (0.171)	9.053 (0.076)
2	NH str	5.211 (0.031)	5.211
3	CH_2 asy str	4.571 (0.069)	4.571
4	CH_2 sym str	4.707 (0.072)	4.707
5	Ring str1	4.607 (0.055)	4.509 (0.029)
6	Ring str2	3.785 (0.118)	3.785
7	NC^{α} str	3.476 (0.058)	3.573 (0.025)
8	Ring def	0.947 (0.038)	0.943 (0.014)
9	CO ib	1.036 (0.037)	1.036
10	NH ib	0.568 (0.012)	0.568
11	CH_2 bend	0.525 (0.006)	0.523 (0.002)
12	CH_2 wag	0.648 (0.014)	0.665 (0.005)

Table 4. (continued)

No.	Coordinates	Set I	Set II
13	CH_2 twist	0.612 (0.005)	0.613 (0.003)
14	CH_2 rock	0.762 (0.024)	0.752 (0.006)
15	CO ob	0.493 (0.012)	0.547 (0.009)
16	NH ob	0.353 (0.018)	0.361 (0.003)
17	Ring tor1	0.096	0.096
18	Ring tor2	0.218	0.218
19	CO str,ring str2	0.732	0.732
20	CO str,ring def	0.219	0.219
21	Ring str1,CH_2 bend	−0.048 (0.036)	−0.048
22	Ring str2,ring def	0.150 (0.037)	0.151 (0.014)
23	NC^{α} str,NH ib	−0.093 (0.029)	−0.093
24	NC^{α} str,CH_2 bend	−0.149 (0.037)	−0.149
25	NC^{α} str,CH_2 wag	0.327 (0.029)	0.327
26	CH_2 rock,NH ob	−0.036 (0.040)	−0.036
27	CO ob,NH ob	0.096 (0.024)	0.096

*Set I was refined for all six isotopes; set II was refined for $(CONHCH_2)_2$ alone. Figure in parentheses is dispersion for refined force constants.

Table 5. Raman intramolecular modes of diketopiperazine, using set I force constants

Observ.* (cm^{-1})	Calc.* (cm^{-1})	Potential energy distribution†
		$(CONHCH_2)_2$
	3121 (0) [0]	NH s(97)
2954 [1]	2953 (0) [0]	CH_2 as(87),CH_2 ss(11)
2929 [0]	2922 (0) [0]	CH_2 ss(87),CH_2 as(11)
1655‡ [−28]	1664 (0) [−29]	CO s(30),Rs1(28),NH ib(17),NC^{α} s(12), Rd2(10)
1519 [−18]	1516 (−1) [−20]	Rs2(50),CO ib(15),NH ib(13),CH_2 b(11)
1457 [−6]	1465 (−1) [−4]	NH ib(46),CH_2 b(28)
1422 [−10]	1418 (5) [−18]	CH_2 b(45),NH ib(16),Rs2(12),CO s(12)
1313 (−6) [−5]	1293 (−2)	CH_2 w(47),CO s(22),CH_2 t(20)
1261 [−2]	1283 (3)	CH_2 t(73),CH_2 w(12)
1149 (−6) [−4]	1156 (−6) [−2]	NC^{α} s(39),CH_2 w(16),CO s(13)
985 [−8]	992 (−5) [−7]	CH_2 r(72)
832 [−1]	819 (0) [0]	NH ob(87)
795 [0]	797 (4) [−1]	Rs1(59),NC^{α} s(13),Rd2(11)
612 [−1]	618 (8) [−1]	CO ib(56),Rs2(28)
561 [−12]	561 (−1) [−11]	CO ob(80),CH_2 r(11),NH ob(11)
473 (−7) [−2]	475 (−7) [−4]	Rd2(67),NC^{α} s(12),Rd1(11)
443 [−2]	444 (6) [−4]	Rd1(71)
236 [0]	296 (−4) [−1]	Rtor (38),CO ob(15),CH_2 r(11)
		$(CONDCH_2)_2$
2954 [−1]	2953 (0) [0]	CH_2 as(87),CH_2 ss(11)
2934 [−5]	2922 (0) [0]	CH_2 ss(87),CH_2 as(11)
2290 [−4]	2290 (0) [0]	ND s(95)
1609‡ [−35]	1645 (0) [−32]	CO s(36),Rs1(31),CH_2 w(13),NC^{α} s(12),Rd2(11)
1508 [−19]	1508 (−1) [−22]	Rs2(46),CH_2 b(20),CO ib(16)
1429 (−7) [−3]	1427 (5) [−11]	CH_2 b(66),Rs2(14)
1323 (−5) [−2]	1293 (−2)	CH_2 w(46),CO s(23),CH_2 t(19)
1259 [−3]	1283 (3)	CH_2 t(74)
1241 [−16]	1243 (−4) [−7]	ND ib(28),NC^{α} s(23),CO s(18),CH_2 w(17)
1008 (−7) [−1]	1011 (−1) [−1]	ND ib(52),NC^{α} s(13)
982 [−5]	989 (−6) [−6]	CH_2 r(62)
787 [−2]	786 (3) [−1]	Rs1(59),NC^{α} s(13),Rd2(11)
626 [−6]	638 (−1) [0]	ND ob(97)
596 [−2]	603 (9) [−1]	CO ib(51),Rs2(26)
537 [−9]	558 (−2) [−11]	CO ob(78),CH_2 r(11)
469 (−5) [−5]	473 (−7) [−5]	Rd2(68),NC^{α} s(14)
437 [−4]	437 (5) [−3]	Rd1(77)
232 [0]	285 (−4) [−1]	Rtor(40),CO ob(14),CH_2 r(11)

Table 5. (continued)

Observ.* (cm^{-1})	Calc.* (cm^{-1})	Potential energy distribution†
		$(CONHCD_2)_2$
	3121 (0)	NH s(97)
2222	2198 (0)	CD_2 as(96)
2130	2144 (0)	CD_2 ss(93)
1645‡	1652 (0)	CO s(32),Rs1(29),NH ib(20),NC^{α} s(13),Rd2(11)
1496	1489 (0)	Rs2(57),CO ib(18),NH ib(18)
1437	1444 (0)	NH ib(55),CO s(20)
1235	1236 (0)	NC^{α} s(44),CO s(34),CD_2 w(15)
1071 (−5)	1074 (0)	CD_2 b(64)
953 (−9)	952 (−5)	CD_2 w(57),CD_2 b(10)
941	925 (3)	CD_2 t(90)
870	865 (−1)	CD_2 r(49),NH ob (23),CO ob(18)
823	812 (−1)	NH ob(68)
757	746 (6)	Rs1(52),NC^{α} s(13)
590	582 (7)	CO ib(49),Rs2(28),CD_2 w(11)
504	488 (−7)	CO ob(64),CD_2 r(26)
468 (−7)	466 (0)	Rd2(61),NC^{α} s(13)
434	438 (5)	Rd1(77)
208	277 (−6)	Rtor(43)
		$(CONDCD_2)_2$
2290	2290 (0)	ND s(95)
2220	2198 (0)	CD_2 as(96)
2135	2144 (0)	CD_2 ss(93)
1607‡	1631 (0)	CO s(40),Rs1(33),NC^{α} s(13),Rd2(13)
1472	1476 (1)	Rs2(63),CO ib(23)
1284	1266 (−1)	CO s(44),NC^{α} s(39),ND ib(12)
1110	1113 (−1)	ND ib(54),CD_2 w(29)
1070 (−5)	1072 (0)	CD_2 b(63)
940	925 (3)	CD_2 t(91)
902 (−11)	895 (−5)	CD_2 w(36),ND ib(21),NC^{α} s(11)
867	859 (−3)	CD_2 r(52),CO ob(20)
750	735 (6)	Rs1(53),NC^{α} s(13)
616	632 (−1)	ND ob(88)
585	574 (9)	CO ib(49),Rs2(27)
495	487 (−7)	CO ob(65),CD_2 r(27)
464 (−9)	465 (−1)	Rd2(61),NC^{α} s(14)
432	432 (5)	Rd1(79)
205	266 (−5)	Rtor(45)

*Figure in parentheses is A_g-B_g splitting ($\nu_A - \nu_B$); figure in brackets is ^{13}C-shift.

†Diagonal elements $\geqslant 10\%$. Abbreviations: s = stretch, as = antisymmetric stretch, ss = symmetric stretch, Rs = ring stretch, Rd = ring deformation, b = bend, w = wag, t = twist, r = rock, Rtor = ring torsion, ib = in-plane bend, ob = out-of-plane bend.

‡Average of A_g, B_g pair.

Table 6. Infrared intramolecular modes of diketopiperazine, using set I force constants

Observ.* (cm^{-1})	Calc.* (cm^{-1})	Potential energy distribution†
		$(CONHCH_2)_2$
	3123 (0) [0]	NH s(96)
2952	2953 (0) [0]	CH_2 as(88),CH_2 ss(10)
	2921 (0) [0]	CH_2 ss(88),CH_2 as(11)
1688‡ [−40]	1695 (0) [−32]	CO s(47),NH ib(24),Rs2(23)
1482 [−8]	1482 (−1) [−12]	NH ib (34),CO s(29),Rs1(16)
1470 [−27]	1477 (0) [−25]	Rs1(55),NH ib(27)
1445 [−2]	1446 (−4) [−3]	CH_2 b(84)
1343 [−2]	1331 (3) [−14]	CH_2 w(63),NC^{α} s(11)
1252 [−2]	1251 (−5) [−1]	CH_2 t(93)
1075 [−7]	1065 (0) [0]	NC^{α} s(74)
993 [−8]	994 (6) [−2]	CH_2 r(74)
913 [−1]	914 (2) [0]	Rd(47),Rs2(42)
837 [−1]	827 (0) [−1]	NH ob(80),Rtor2(11)
805 [−3]	802 (4) [−3]	Rs2(31),Rd(28),CO s(16)
553 [−6]	528 (−4) [−13]	CO ob(89)

Table 6. (continued)

Observ.* (cm^{-1})	Calc.* (cm^{-1})	Potential energy distribution†
447 [−1]	447 (16) [0]	CO ib(56)
285	314 (3) [0]	Rtor1(35)
177	181 (−12) [0]	Rtor2(48)
		$(CONDCH_2)_2$
2952 [0]	2953 (0) [0]	CH_2 as(88),CH_2 ss(10)
2922 [2]	2921 (0) [0]	CH_2 ss(88),CH_2 as(11)
	2296 (0) [0]	ND s(95)
1668‡ [−31]	1663 (0) [−41]	CO s(63),Rs2(24)
1469 [−22]	1478 (0) [−25]	Rs1(64),CH_2 w(12),CO ib(11)
1447 [0]	1447 (−3) [−4]	CH_2 b(85)
1351 [−4]	1343 (3) [−14]	CH_2 w(48),Rs1(16),CO s(12)
1253 [−2]	1251 (−5) [−1]	CH_2 t(93)
1235 [−11]	1235 (−1) [−3]	NC^{α} s(44),ND ib(44),CH_2 w(13)
990 [−7]	991 (1) [−2]	CH_2 r(69)
969 [−2]	988 (9) [−1]	NC^{α} s(34),ND ib(14),Rs2(10)
888 [0]	871 (2) [0]	Rd(60),Rs2(15),ND ib(11)
778 [−4]	764 (2) [−2]	Rs2(42),ND ib(16),Rd(12),CO s(10)
661 [−6]	668 (1) [−3]	ND ob(87),CO ob (19)
510 [−7]	511 (−3) [−11]	CO ob(73)
444 [−1]	444 (15) [0]	CO ib(55),Rs1(10)
	293 (4) [0]	Rtor1(37),CH_2 r(11)
	178 (−13) [0]	Rtor2(49)
		$(CONHCD_2)_2$
	3123 (0)	NH s(96)
2220	2198 (0)	CD_2 as(96)
	2142 (0)	CD_2 ss(94)
	1684 (0)	CO s(51),NH ib(24),Rs2(22)
1479	1478 (0)	NH ib(60),CO s(24)
1466	1457 (−2)	Rs1(71),CO ib(15)
1189	1195 (0)	CD_2 w(45),NC^{α} s(38),Rs2(14)
1077	1079 (−1)	CD_2 b(71),NC^{α} s(11)
1005	992 (−4)	NC^{α} s(35),Rs2(12),CD_2 w(10)
930	927 (−3)	CD_2 t(74),NH ob(21)
885?	850 (2)	CD_2 r(33),NH ob(25),CD_2 t(11),Rd(10)
843?	832 (5)	Rd(50),CD_2 b(12),NH ob (10)
827?	777 (3)	CD_2 r(36),NH ob(29),CO ob(13)
737	728 (5)	Rs2(41),CD_2 w(31)
485	487 (−4)	CO ob(78),CD_2 r(10)
440	442 (16)	CO ib(54),Rs1(10)
	279 (1)	Rtor1(36)
	180 (−10)	Rtor2(48)
		$(CONDCD_2)_2$
	2296 (0)	ND s(95)
2228	2198 (0)	CD_2 as(96)
	2142 (0)	CD_2 ss(94)
	1652 (0)	CO s(70),Rs2(23),Rd(11)
1462	1455 (0)	Rs1(79),CO ib(14)
1238	1255 (−1)	ND ib(47),Rs2(14),CO s(13),NC^{α} s(11)
1182	1182 (0)	NC^{α} s(51),CD_2 w(43),CO ib(11)
1067	1065 (−2)	CD_2 b(79)
930	918 (−4)	CD_2 t(87)
890?	881 (0)	ND ib(33),NC^{α} s(27),CD_2 w(15)
838?	831 (9)	Rd(41),CD_2 r(26)
872?	809 (2)	CD_2 r(47),Rd(22)
729	711 (3)	Rs2(47),CD_2 w(26)
645	651 (0)	ND ob(78), CO ob(18)
460	467 (−3)	CO ob(63)
438	439 (14)	CO ib(51)
	265 (3)	Rtor1(38)
	177 (−12)	Rtor2(49)

*Figure in parentheses is A_u-B_u splitting ($\nu_A - \nu_B$); figure in brackets is ^{13}C-shift.

†Diagonal elements $\geqslant 10\%$. Abbreviations: s = stretch, as = antisymmetric stretch, ss = symmetric stretch, Rs = ring stretch, Rd = ring deformation, b = bend, w = wag, t = twist, r = rock, Rtor = ring torsion, ib = in-plane bend, ob = out-of-plane bend.

‡Average of A_u, B_u pair.

Table 7. Intramolecular modes of $(CONHCH_2)_2$, using set II force constants

Observ.* (cm^{-1})	Calc.* (cm^{-1})	Potential energy distribution†
Raman		
	3121 (0)	NH s(97)
2952	2952 (−1)	CH_2 as(87),CH_2 ss(11)
2922	2921 (−1)	CH_2 ss(87),CH_2 as(11)
1655‡	1657 (0)	Rs1(28),CO s(26),NH ib(16),CH_2 w(15),NC^{α} s(12)
1521	1521 (0)	Rs2(43),NH ib(22),CH_2 b(11),CO ib(10)
1457	1457 (−1)	NH ib(39),CH_2 b(36),CH_2 w(10)
1422	1421 (5)	CH_2b(38),Rs2(16),NH ib(16),CO s(13)
1313 (−6)	1313 (−4)	CH_2 w(56),CO s(26)
1261	1261 (5)	CH_2 t(92)
1149 (−6)	1148 (−5)	NC^{α} s(44),CO s(19)
985	985 (−5)	CH_2 r(71)
832	832 (0)	NH ob(87)
795	795 (4)	Rs1(58),NC^{α} s(14),Rd2(11)
612	613 (9)	CO ib(56),Rs2(27)
561	561 (−2)	CO ob(78),CH_2 r(11)
473 (−7)	473 (−7)	Rd2(66),Rd1(13),NC^{α} s(11)
443	442 (5)	Rd1(69),NC^{α} s(11)
236	296 (−4)	Rtor(38),CO ob(15),CH_2 r(12)
Infrared		
	3123 (0)	NH s(96)
2952	2953 (0)	CH_2 as(88),CH_2 ss(10)
	2921 (0)	CH_2 ss(88),CH_2 as(11)
1688‡	1693 (0)	CO s(45),NH ib(24),Rs2(23)
1482	1480 (0)	NH ib(52),CO s(33)
1470	1470 (0)	Rs1(65),CH_2 w(16)
1445	1445 (−4)	CH_2 b(84)
1343	1342 (3)	CH_2 w(57),Rs1(13),CO ib(11),NC^{α} s(11)
1252	1252 (−5)	CH_2 t(93)
1075	1075 (0)	NC^{α} s(73)
993	992 (7)	CH_2 r(74)
913	914 (2)	Rd(47),Rs2(43)
837	836 (0)	NH ob(80),Rtor2(10)
805	802 (5)	Rs2(30),Rd(29),CO s(16)
553	553 (−3)	CO ob(87)
447	447 (16)	CO ib(56),Rs1(10)
285	314 (3)	Rtor1(35)
177	181 (−12)	Rtor2(48)

*Figure in parentheses is A-B splitting ($\nu_A - \nu_B$).

†Diagonal elements $\geqslant 10\%$. Abbreviations: s = stretch, as = antisymmetric stretch, ss = symmetric stretch, Rs = ring stretch, Rd = ring deformation, b = bend, w = wag, t = twist, r = rock, Rtor = ring torsion, ib = in-plane bend, ob = out-of-plane bend.

‡Average of A, B pair.

sets of intermolecular potentials will then be examined. Finally, we will consider the special problem of the CO str modes.

Force constants

Our force constants are well determined, as shown by the dispersions. This, and the favorable ratio of parameters to observed data (approximately 31 : 80 in the g block, and 27 : 70 in the u block), may be attributed to our refinement procedure. The use of a non-redundant basis removed fundamental correlation among the force constants and reduced the number of terms needed. Defining local symmetry coordinates reduced accidental correlation as well by making several modes dependent mainly on only one or two diagonal force constants, in particular, the methylene deformations, and CO and NH in-plane bends. The ring coordinates were also constructed with this aim in mind. For example, the CN and $C^{\alpha}C$ stretches appear in the Ring stretches as $CN \pm C^{\alpha}C$; this was done in view of the experimental conclusion that these two bond stretches are strongly coupled, a feature borne out by the calculations. Finally, separation of the coordinates into symmetry species, while reducing further the number of force constants, is also advantageous when the data for different symmetry blocks are not of the same completeness and accuracy, as is the case with our Raman and i.r. data. We may mention that the use of local symmetry force constants is quite common [22], and in the case of small highly symmetric molecules force constants are often refined in non-redundant group symmetry coordinates speci-

fic to each molecule (e.g. [23]); non-redundant coordinates for a molecule like DKP necessarily assume more complicated forms.

The latest poly(glycine I) force field of DWIVEDI and KRIMM [21] was refined in a redundant primitive internal coordinate basis. However, it is possible to compare most of our diagonal force constants to the PGI set when the latter is transformed to a local symmetry basis. To make this comparison, we take the average of the *g* and *u* values for DKP, with the following results (PGI values in parentheses)—NH str: 5.211 (5.840), CH_2 as: 4.571 (4.554), CH_2 ss: 4.707 (4.574), CO ib: 1.255 (1.246), NH ib: 0.563 (0.521), CH_2 b: 0.519 (0.531), CH_2 w: 0.673 (0.688), CH_2 t: 0.617 (0.673), CH_2 r: 0.658 (0.711), CO ob: 0.505 (0.587), NH ob: 0.349 (0.129).

It can be seen that the values for DKP are not drastically different from those for the *trans* peptide, except for the NH ob parameter. We hope to calculate the DKP force field by *ab initio* molecular orbital methods in the near future; having our empirical set in a non-redundant basis will facilitate comparison with the *ab initio* set [24]. Finally, we are attempting to transfer the DKP force field to other cyclic dipeptides; where coordinates similar to those in DKP can be defined, the force constants can be used as they are; in other cases, the DKP set can be transformed to the required basis.

Intramolecular modes

Most of the discrepancies between observed frequencies and the values calculated with Set I force constants are less than 10 cm^{-1}, though a few are between 20 and 30 cm^{-1}. (The three ring torsional modes were not fitted because of uncertainty in the assignment of the far i.r. bands and because of high sensitivity to the intermolecular potential, as noted earlier.) These remaining errors are undoubtedly due mainly to the neglect of minor interaction terms and to the use of data on several isotopes without allowing for anharmonicity. The frequency agreement using Set II is essentially exact.

An internal coordinate description of normal modes is not always convenient or informative, especially for highly delocalized vibrations. We therefore present in Figs 2 and 3 the atomic displacements in each intramolecular mode of DKP (except the XH stretches) computed with Set II force constants. In these figures (drawn with ORTEP) the oxygen atoms are drawn extra large and the frequencies are the calculated ones listed in Table 7. In all modes the molecule is rotated so that the largest amplitude motions are shown clearly.

Beginning with the Raman modes, it is striking how delocalized most of the vibrations are. At one extreme CH_2 twist (1261) is perfectly localized on the methylene hydrogens and at the other extreme the two Ring def (473 and 442) and the Ring tor (296) modes involve equally large motions of all 14 atoms. It seems that only the NH ob mode (832) can be considered to be a pure vibration of the peptide group.

As is already evident from the internal coordinate PEDs, NH ib is a component in all the four modes in the 1400–1700 cm^{-1} region. What is not obvious from the PEDs is that the amplitude of the NH vibration is among the largest in each mode, even when it contributes only a small fraction of the total potential energy. This illustrates the hazard of characterizing a mode using its PED alone.

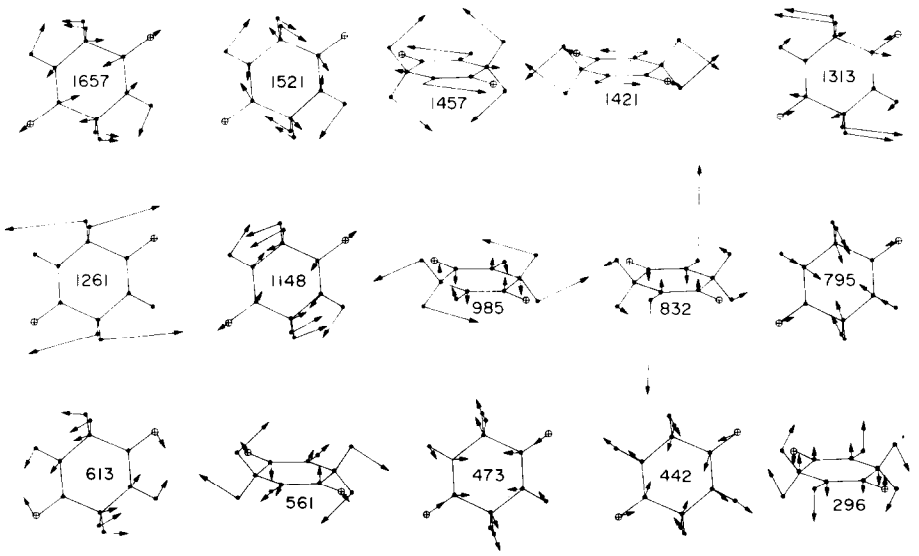

Fig. 2. Raman-active intramolecular modes of DKP.

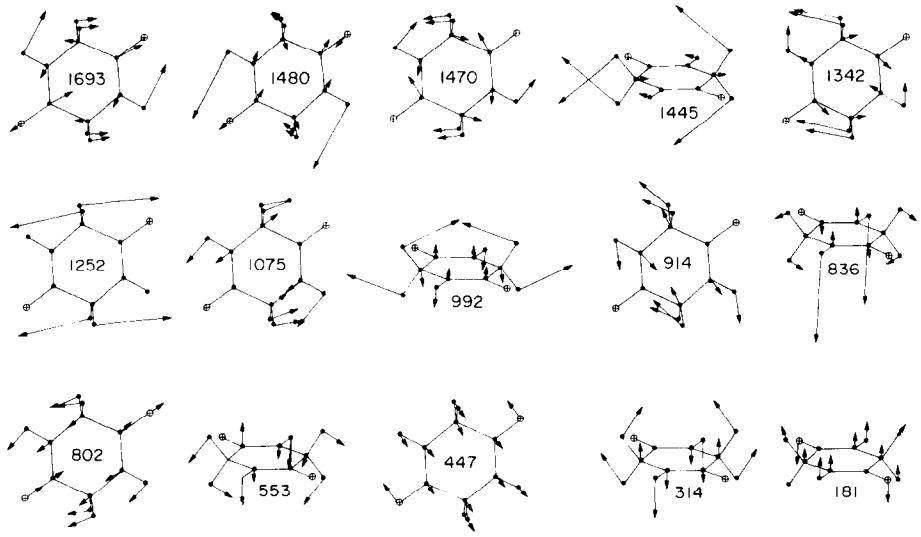

Fig. 3. Infrared-active intramolecular modes of DKP.

The description of the 1521 cm^{-1} mode as out-of-phase $C^{\alpha}CN$ str is nicely shown, and the 1457 and 1421 cm^{-1} modes can be seen to involve in-phase and out-of-phase bending of adjacent CH_2 and NH groups. Another in-phase/out-of-phase relationship is seen with CH_2 rock and CO ob in the 985 and 561 cm^{-1} modes. The strong tendency of NC^{α} str to couple with CD_2 wag and ND ib is apparent in the large motions of the NH and CH_2 groups in the 1148 cm^{-1} mode. Finally, the 795, 473 and 442 cm^{-1} modes display an interesting similarity: groups on opposite sides of the ring move toward each other.

Turning to the i.r. modes, we again find CH_2 twist (1252) to be the most localized mode. The 1693 and 1480 cm^{-1} modes involve in-phase and out-of-phase vibrations of CO str and NH ib. The 1470 cm^{-1} mode is out-of-phase $C^{\alpha}CN$ str with a large NH ib amplitude, even though the potential energy of the latter is less than 10%.

The 1075 cm^{-1} mode is a well-localized vibration of the $NHCH_2$ groups (which may be contrary to observation since it shows a significant ^{13}C shift). So too is the 914 cm^{-1} mode; this is very similar to the 795 cm^{-1} Raman mode, but with opposite phases of adjacent NH and CH_2 fragments.

The ring torsional modes (181 and 314) are, as expected, highly delocalized vibrations. There are some differences between them that may account for one being observed only in i.r. absorption and the other only in neutron scattering (according to our tentative assignments). The 314 cm^{-1} mode has large H atom amplitudes, consistent with its assignment to the 285 cm^{-1} neutron peak. (Incidentally, the 296 cm^{-1} Raman mode also has large motions of the H atoms, so that its correlation with the strong 215 cm^{-1} neutron peak is reasonable.) If we take the charge distribution of the molecule to be such that the H atoms and the carbonyl C atom are positive and the N, O and C^{α} atoms are negative (consistent with the partial charges in the atom–atom potentials of both HAGLER *et al.* and MOMANY *et al.*), the 181 cm^{-1} mode may be expected to have a larger transition dipole moment than the 314 cm^{-1} mode.

The possible use of atomic displacements in qualitatively estimating i.r. intensities is an advantage of cartesian over internal coordinate eigenvectors. For instance, it is now clear from the PEDs why the 1693 and 1480 cm^{-1} modes should have such different intensities. The atomic displacements show that in one the transition moments of the CO and NH groups add up, whereas in the other they subtract from each other. Similar considerations can account for the low intensities of the CH_2 twist (1252), CH_2 rock (992) and CO ob (553) modes.

With the detailed understanding of the normal modes of DKP gained from experiment and calculations, we may not consider the problem of extending our results to other molecules. We are particularly interested in identifying modes characteristic of the *cis* CONH group, that is, modes that are more or less localized on CONH and are different from those of *trans* structures.

It seems that the NH ob mode is the most suitable. Its position in the 800 cm^{-1} region contrasts with that of the *trans* amide V ($\sim$ 700 cm^{-1}). It is strong (at least in the i.r.) and can be identified easily by deuteration. Not only is it highly localized on NH, but its frequency and character are almost identical in both the Raman and i.r. This second point is important because it implies that this mode does not depend on the special symmetry present in DKP; in other words, there is little interaction between the two peptide groups in this mode, either directly or via the CH_2 groups.

A few other modes may be considered to be approximately localized on the CONH fragments. Examples are the i.r. NH ib and CO ib modes.

However, the corresponding vibrations are very different in frequency and in character in the Raman. They may be expected to be characteristic of cyclic dipeptides, but probably cannot be extended to linear *cis* peptides. We should emphasize again that one of the conventional criteria for identifying a *cis* peptide, namely, the absence of a band in the 1500 cm^{-1} region [25, 26], is not always valid.

Lattice modes and intermolecular potentials

The lattice modes for all six isotopes calculated with MOMANY *et al.*'s [10] atom–atom potentials (and Set I intramolecular force constants) are given in Table 8. We also list in Table 9 the results of calculations on DKP alone using Set II and different sets of atom–atom potentials: those of MOMANY *et al.* [10], HAGLER *et al.* [7, 8] and DASHEVSKY [27, p. 391]. MOMANY *et al.*'s set consists of 6-12-1 terms. Since the atomic charges in the Coulombic part were derived quantum mechanically by CNDO/2 methods, independently of the 6-12 terms, we think it is justified to use only the 6-12 part.

For completeness we list in Table 10 the parameters of these potentials. (MOMANY *et al.*'s special 10-12 hydrogen bond potential is not listed since we did not use it.) Only the parameters for like-atom interactions are given; unlike-atom parameters are given by combining rules. In HAGLER *et al.*'s set, the rules for their attractive (A) and repulsive (B) coefficients are:

$$A_{ij} = (A_{ii}A_{jj})^{1/2},\ B_{ij} = (B_{ii}B_{jj})^{1/2}.$$

DASHEVSKY's rules for A, B and the exponential (C) parameter in the 6-exp form are:

$$B_{ij} = \tfrac{1}{4}(B_{ii}^{1/2} + B_{jj}^{1/2})^2,\ C_{ij} = \frac{2C_{ii}C_{jj}}{C_{ii}C_{jj}},$$

$$A_{ij} = 23.63\ B_{ij}/C_{ij}^{6}.$$

MOMANY *et al.*'s A and B coefficients are obtained from the quantities α, N and ρ in the table by using the

Table 8. Lattice modes (in cm^{-1}) using MOMANY *et al.*'s potentials with no Coulombic terms*.

	A_g	B_g	A_u	B_u
$(CONHCH_2)_2$	132 (142)	151 (159)	54 (83)	127 (148)
	127 (126)	129 (126)	41 (47)	
	70 (51)	64 (67)		
$(CONDCH_2)_2$	128 (140)	149 (157)	54	126
	122 (123)	122 (123)	40	
	69 (51)	63 (67)		
$(CONHCD_2)_2$	129 (138)	148 (155)	53	125
	123 (123)	125 (123)	40	
	68 (49)	61 (66)		
$(CONDCD_2)_2$	126 (136)	146 (153)	53	124
	120 (121)	120 (121)	40	
	67 (49)	61 (64)		
$(^{13}CONHCH_2)_2$	131 (141)	151 (159)	54	126
	126 (125)	128 (125)	40	
	70 (51)	63 (67)		
$(^{13}CONDCH_2)_2$	128 (138)	149 (155)	53	125
	122 (122)	122 (122)	40	
	69 (49)	63 (64)		

*Observed value in parentheses.

Table 9. Comparison of lattice modes (in cm^{-1}) of $(CONHCH_2)_2$ calculated with various sets of atom–atom potentials

	Obs.	MOMANY *et al.* 6-12	MOMANY *et al.* 6-12-1	HAGLER *et al.* 6-12-1	DASHEVSKY 6-exp
A_g	142	132	137	177	114
	126	127	134	162	107
	51	70	78	103	61
B_g	159	151	158	184	123
	126	129	136	177	111
	67	64	71	99	61
A_u	83	54	52	50	50
	47	41	42	42	35
B_u	148	127	127	129	112

Table 10. Atom–atom potential parameters

		O	C	H(N)	N	C^{α}	$H(C^{\alpha})$
MOMANY *et al.*	q	−0.384	0.450	0.176	−0.344	−0.009	0.055
6-12-1	$\alpha \times 10^{24}$	0.84	1.51	0.42	0.87	0.93	0.42
	N	7.00	5.20	0.85	6.10	5.20	0.85
	ρ	3.12	3.74	2.68	3.99	4.12	2.92
HAGLER *et al.*	q	−0.38	0.38	0.28	−0.28	−0.20	0.10
6-12-1	A	502	1340	0	1230	532	32.9
	$B \times 10^{-3}$	275	3022	0	2271	1811	7.15
DASHEVSKY	A	354	476	40.1	395	476	40.1
6-exp	$B \times 10^{-4}$	9.65	3.77	2.86	7.62	3.77	2.86
	C	4.333	3.513	5.200	4.063	3.513	5.200

following relations:

$$A_{ij} = 3.6235 \times 10^{38} \alpha_i \alpha_j / ((\alpha_i/N_i)^{1/2} + (\alpha_j/N_j)^{1/2})$$

$$B_{ij} = A_{ij} \rho_{ij}^6 / 2$$

$$\rho_{ij} = (\rho_i + \rho_j)/2.$$

(MOMANY *et al.*'s paper should be referred to for the derivation of these expressions.) The Coulombic interaction between atoms i and j in HAGLER *et al.*'s set is simply $332\, q_i q_j / r$; and in MOMANY *et al.*'s it is given by $332\, q_i q_j / 2r$, a dielectric constant of 2 being assumed. The factor of 332 converts the energy to kcal/mole when q is in electronic charge units and r in Å. The units of the other parameters are such as to yield the energy in kcal/mole. Multiplication of the energy by 6.9473×10^{-3} converts it to mdyne-Å, so that the force constant is obtained in mdyne/Å. We used an interaction radius of 5 Å. This was sufficient for convergence.

While there is little difference in the performance of the potentials in the case of the A_u and B_u lattice modes (whose assignments are not definitive anyway), the results for the rotatory modes are very different. In particular, HAGLER *et al.*'s 6-12-1 potentials give frequencies that are consistently much too high. MOMANY *et al.*'s potentials are clearly the best, and we prefer his 6-12 set for best overall performance. One of our central experimental conclusions, that an A_g mode is overlapped with a B_g at 126 cm^{-1}, is nicely substantiated when MOMANY *et al.*'s parameters are used but is not reflected in calculations with HAGLER *et al.*'s (unless one reverses the order of the 177 and 162 cm^{-1} A_g modes, an assignment that is not in accord with X-ray data, which we consider below). It is difficult to say whether the remaining discrepancies between experimental frequencies and those calculated with MOMANY *et al.*'s 6-12 or 6-12-1 parameters can be removed by an improved treatment of the lattice dynamics (i.e. minimization of the crystal energy and inclusion of the "linear term"). This is the subject of future work.

We now look more closely at the nature of the lattice modes obtained with MOMANY *et al.*'s 6-12 set. Since a cartesian eigenvector description is the most appropriate for such modes, we present in Fig. 4 the atomic displacements in each lattice mode. The rotatory and translatory nature of the modes is vividly shown.

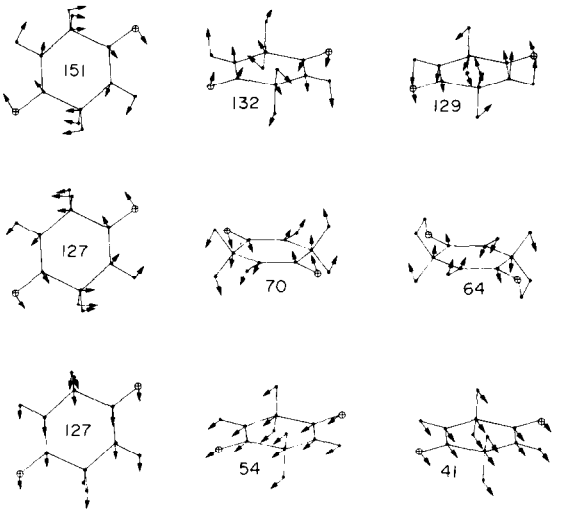

Fig. 4. Lattice modes of DKP.

The 151 and 127 cm^{-1} Raman modes are obviously rotations about the normal to the molecular plane, one being the in-phase and the other the out-of-phase vibration of the two molecules in the unit cell. An analysis by LONSDALE [28] of the anisotropic heavy atom X-ray thermal parameters of DM [11] shows that this axis is indeed a libration axis. She obtained a root-mean-square rotational amplitude of 1.8° about this axis.

CRUICKSHANK [29] has given an approximate relation between the mean-square librational amplitude and the normal mode frequencies for the case of two molecules per unit cell, which we may write as

$$\langle \phi_i^2 \rangle = \frac{k_B T}{8\pi^2 c^2 I_i} \left(\frac{1}{\nu_1^2} + \frac{1}{\nu_2^2} \right) (\text{rad}^2)$$

where I_i is the moment of inertia about the ith axis and ν_1 and ν_2 are the in-phase and out-of-phase frequencies. The assumptions are that the temperature T is sufficiently high, and the dispersion relations of the ν_1 and ν_2 modes are independent of the wavevector. We estimated the moment of inertia about the axis

normal to the molecular plane as $I_i = 406.15$ amu-Å^2 $= 6.7443 \times 10^{-38}$ g-cm^2. Using $T = 300$ K and the observed frequencies of 159 and 126 cm^{-1}, we compute $\langle \phi_i^2 \rangle^{1/2}$ to be 1.71°. The excellent agreement with the X-ray result confirms our assignment of the calculated 151 and 127 cm^{-1} modes and is also an indication of the appropriateness of MOMANY *et al.*'s potentials. (The 162 cm^{-1} A_g mode obtained with HAGLER *et al.*'s parameters is a libration about the normal to the molecular plane and therefore should be correlated with the observed 126 cm^{-1} A_g mode.)

The other two libration axes are expected to be orthogonal to each other in the molecular plane, but their precise orientations are not easily deduced from the atomic displacements without a perhaps tedious geometrical analysis. One of the axes seems to be approximately along [101] as suggested by the 70 and 64 cm^{-1} modes. LONSDALE's analysis did indicate [101] to be a possible axis, but unfortunately she dismissed it in favor of another pair of axes one of which is 45° from [101] in the direction of the CO bond. It may be possible to repeat her analysis to obtain the amplitudes about axes conforming to our results, but we will not do so here.

The translatory modes are along b (127 cm^{-1}) and approximately along c (54 cm^{-1}) and a (41 cm^{-1}). The b translation axis agrees with LONSDALE's results but she determined the other two axes to be [101] and $\perp$ $(10\bar{1})$.

Finally, we consider the factor group splittings obtained with MOMANY *et al.*'s 6-12 parameters and the Set II intramolecular force field. We observe only three *A-B* splittings for DKP (aside from the CO stretches), all of them in the Raman. Table 7 shows that each splitting is reproduced very well. However, there are several sizeable splittings predicted in each block that are not observed. Probably many, if not most, of the discrepancies are due to insufficient instrument resolution or insufficient intensity of the other component. Nevertheless, a few instances are difficult to explain. For example, our single crystal spectra of DKP show strong A_g and B_g intensity for some modes, such as CO ib (612) and CH_2 twist (1261), which are calculated to have significant splittings comparable to those that we did measure. Yet our data did not show any difference in position between these A_g and B_g bands.

In summary, it seems that MOMANY *et al.*'s 6-12 potential gives results in good agreement with observations. Discrepancies such as in the A_u and B_u lattice mode frequencies and in certain *A-B* splittings may be due to experimental uncertainty as well as to deficiencies in the potential and dynamical models. It is fortunate that we find the 6-12 form to be somewhat better than the full 6-12-1 form since the Coulombic part requires atomic charges to be determined for each molecule. Because this set of parameters was determined not for DKP alone but for a large class of amides (and hydrocarbons), we may recommend this set for normal mode analysis of peptide crystals. Note, however, that special attention should be given to the hydrogen bond H . . . O interaction, for which we had to assume an arbitrary value of 0.150 mdyne/Å.

Problem of CO stretch modes

There are two sets of prominent splittings of the CO str modes observed in the solid state: the *A-B* splittings in both Raman and i.r., and the *g-u* splittings between Raman and i.r. We tabulate these splittings (in cm^{-1}) in Table 11 for the six isotopes, with calculated *g-u* values in parentheses.

In all cases $\nu_u > \nu_g$ and in the Raman $\nu_B > \nu_A$; no symmetry assignment is available for the i.r. bands. The *g-u* splittings are taken between the ν_A, ν_B average values, except in the ^{13}C compounds where no Raman *B* component was measured.

The only splittings we have been able to reproduce with our force field are the *g-u* splittings for DKP and C13DKP. This was accomplished by refining the force constants for the *g* and *u* blocks separately. As we noted in paper 1 [1], the frequency difference between the *g* and *u* modes arises from an interaction between CO groups related by the inversion operation. We obtained f(CO str) values of 7.619 and 9.125 mdyne/Å in the *g* and *u* blocks (Set I), which implies an interaction force constant of -0.753 mdyne/Å between CO str coordinates. Because the coordinates are crystal symmetrized, the interaction represented by this force constant can be between CO stretches on different molecules, in particular molecules in a hydrogen bonded chain.

Of the two proposed explanations of the *g-u* splitting in structures like ours, viz. transition dipole coupling [30] and dynamical charge transfer [31], both of which lead to interactions between the CO groups, the latter seems to be favored as the predominant mechanism in DKP. It is clear from Figs 2 and 3 that the CO str modes are delocalized over the entire molecule. It is not reasonable then to assume transition dipoles localized on each CO bond, or even on a peptide group. Instead, the transition moments should be associated with the entire molecule. It is then impossible to explain any *g-u* splitting by considering dipole–dipole interactions between molecules along a chain: the molecules are all translationally equivalent and such interactions will not lead to any splitting. We may mention that the need to consider molecule-centered rather than bond- or fragment-centered

Table 11. Prominent splittings of CO str modes observed in the solid state

	Raman *A-B*	*g-u*	i.r. *A-B*
$(CONHCH_2)_2$	19	33 (31)*	19
$(CONDCH_2)_2$	15	59 (18)	26
$(CONHCD_2)_2$	13	— (32)	—
$(CONDCD_2)_2$	11	— (21)	—
$(^{13}CONHCH_2)_2$	—	−28 (28)	19
$(^{13}CONDCH_2)_2$	—	−60 (9)	23

*Calculated values in parentheses.

transition dipoles would explain the absence of any significant observed g-u splitting in D_2O solution.

BOSI *et al.* [31] obtained by an *ab initio* calculation a CO str, CO str interaction term of -0.3 mdyne/Å in formic acid dimer, a term that was said to arise from transfer of charge in the cyclic hydrogen bond structure during the vibration. This resulted in a g-u splitting of 20 cm^{-1} compared to the observed value of 69 cm^{-1}. Our value of -0.753 mdyne/Å for the interaction in DKP is therefore not unreasonably large.

The large increase in the g-u splitting in NdDKP and NdC13DKP can also be attributed to the charge transfer mechanism. With the decrease in NH ib contribution to the mode the proportion of CO str increases. The magnitude of the charge transfer is also expected to increase, leading to a larger interaction and hence a larger splitting. This implies that to reproduce the g-u splitting in the N-deuterated molecules we would have to allow for CO str force constants different from those in the NH molecules.

Turning to the A-B splittings, the failure of any of the atom–atom potentials to account for the data is conspicuous. Since these potentials were derived from static structural data, they do not incorporate any dynamical effects. We think that resonance interactions in the form of transition multipole terms can provide a reasonable explanation for the A-B splittings.

The i.r. CO str mode has a large transition dipole moment, as is evident from its intensity. As a first approximation, we take this transition dipole to be parallel to the CO bond and located at the inversion center of the molecule. Considering the normal coordinate Q of the mode on two molecules m and n, the transition dipole–transition dipole interaction force constant is [20, 30]:

$$F^Q_{mn} = 0.1\,(\partial\mu/\partial Q)^2\, X_{mn}$$

where X_{mn} is the geometrical factor,

$$X_{mn} = (\hat{e}_m \cdot \hat{e}_n - 3(\hat{e}_m \cdot \hat{r}_{mn})(\hat{e}_n \cdot \hat{r}_{mn}))/r^3_{mn}$$

F^Q_{mn} is given in mdyne/Å (amu) when r_{mn} is in Å and $\partial\mu/\partial Q$ is in D/A $(amu)^{1/2}$. This interaction causes a change in the diagonal force constant associated with the Q mode in each symmetry block. The resulting frequency change is given approximately by

$$\Delta\nu = \frac{N_A 10^5}{8\pi^2 c^2 \nu} F^Q_{mn} = \frac{848\,619}{\nu} F^Q_{mn}\ (cm^{-1}).$$

This follows from the relation $4\pi^2c^2\nu^2 = \lambda$ where λ is the force constant in the normal coordinate basis.

Since the A-B splitting arises from interactions between molecules related by the $C_2^s(b)$ operation, only such interactions need to be considered. The geometrical factor was computed for a given m and all n within a radius of about 30 Å. The result is $\sum_n X_{mn} = -0.0288$. The shift of the mode in DKP, using $\nu = 1688\ cm^{-1}$, is $\Delta\nu = -1.448 \times (\partial\mu/\partial Q)^2$. Taking into account the opposite phases of the two molecules in the unit cell in the A_u and B_u modes, the magnitude of the splitting is 2.896 $(\partial\mu/\partial Q)^2$. The value of $\partial\mu/\partial Q$ implied by a splitting of 19 cm^{-1} is 2.56 D/Å $(amu)^{1/2}$. A preliminary *ab initio* MO calculation on DKP with an STO-3G basis gives a value of 2.37 D/Å $(amu)^{1/2}$. (We will report our *ab initio* results on dipole moment derivatives with the minimal as well as an extended basis set in a forthcoming paper.) Interestingly, the sign of the interaction results in the B_u component being higher in frequency, tending to support our interpretation of the data [1].

In NdDKP, the splitting of 26 cm^{-1} can be fitted with a $\partial\mu/\partial Q$ of 2.98, if we assume the same dipole orientation and location; this is consistent with the higher relative intensity of the band (compare Figs 1(b) and 2(b) of paper 1 [1]).

Thus, transition dipole interaction is a plausible explanation of the A_u-B_u splittings. In the Raman, however, there is clearly no molecular transition dipole associated with the modes. Therefore, it seems that to reproduce the A_g-B_g splittings, we need to invoke quadrupole–quadrupole and higher-order terms. Since the parameters of these higher-order transition moments are not easily estimated except by an *ab initio* calculation, we will not attempt a detailed analysis here. We may point out that if we consider CO bond-centered transition dipoles, as has been done for polypeptides [20], reasonable values for the dipole parameters fail to reproduce the Raman splittings, even though the A_u-B_u splittings can be fitted.

CONCLUSIONS

Our Raman and i.r. [1] data and assignments of crystalline DKP and five of its isotopic derivatives have formed the basis for the refinement of an intramolecular force field for this molecule. This force field is given in a non-redundant basis specially constructed to reduce correlation among the force constants so that fewer parameters are needed. The effectiveness of this procedure is shown by the good overall fit to the data. We have refined two sets of force constants, one to fit the data on all six isotopic species and the other adjusted to give a best fit for DKP alone.

Our analysis shows that one of the criteria used to identify a *cis* peptide group, viz. the absence of a band in the 1500 cm^{-1} region, may not always be valid. In DKP such a band is absent from the i.r. but present in the Raman spectrum. A more suitable criterion may be the observation of the NH out-of-plane bend mode in the 800 cm^{-1} region, as compared to the 700 cm^{-1} region for the *trans* peptide group.

In comparing the effectiveness of various atom–atom potential functions, we find that MOMANY *et al.*'s [10] set gives the best agreement with observed lattice frequencies and internal mode splittings. These parameters, therefore, may be useful in normal mode calculations on other peptide crystals.

Various splittings are found in the Raman and i.r. CO str bands, none of which are predicted by the atom–atom interactions. The large splittings between the Raman CO str and the i.r. CO str modes cannot be explained by a transition dipole coupling mechanism [20, 27], since molecule-centered transition moments are on translationally equivalent molecules. Charge transfer around the hydrogen-bonded ring provides a reasonable mechanism [31] for explaining this splitting. Although such a mechanism cannot account for the i.r. band splittings, we find that transition dipole coupling can reproduce the observations. The Raman band splittings would seem to require transition quadrupole interactions.

Our vibrational analysis of DKP provides a sound basis for understanding the spectra and interactions of this molecule in the crystalline state and we hope will be a useful starting point for similar analyses of other *cis* peptide groups.

Acknowledgements—We are indebted to Prof. ROBERT C. TAYLOR for helpful discussions. This research was supported by National Science Foundation grants PCM-7921652 and DMR-7800753.

REFERENCES

[1] T. C. CHEAM and S. KRIMM, *Spectrochim. Acta* **40A**, 481 (1984).
[2] P. GRONER and HS. H. GÜNTHARD, *J. Molec. Spectrosc.* **61**, 151 (1976).
[3] D. STEELE, *Theory of Vibrational Spectroscopy*. W. B. Saunders, Philadelphia (1971).
[4] G. ZERBI, in *Vibrational Spectroscopy—Modern Trends*, (edited by A. J. BARNES and W. J. ORVILLE-THOMAS). Elsevier, Amsterdam (1977).
[5] T. L. STARR and D. E. WILLIAMS, *Acta crystallogr.* **A33**, 771 (1977).
[6] S. KRIMM, *Biopolymers* **22**, 217 (1983).
[7] A. T. HAGLER, E. HULER and S. LIFSON, *J. Am. chem. Soc.* **96**, 5319 (1974).
[8] A. T. HAGLER and S. LIFSON, *J. Am. chem. Soc.* **96**, 5327 (1974).
[9] F. A. MOMANY, L. M. CARRUTHERS, R. T. MCGUIRE and H. A. SCHERAGA, *J. phys. Chem.* **78**, 1595 (1974).
[10] F. A. MOMANY, L. M. CARRUTHERS and H. A. SCHERAGA, *J. phys. Chem.* **78**, 1621 (1974).
[11] R. DEGEILH and R. E. MARSH, *Acta crystallogr.* **12**, 1007 (1959).
[12] H. A. SCHERAGA, *Biopolymers* **20**, 1877 (1981).
[13] A. T. HAGLER, P. S. STERN, R. SHARON, J. M. BECKER and F. NAIDER, *J. Am. chem. Soc.* **101**, 6842 (1979).
[14] W. C. HAMILTON and J. A. IBERS, *Hydrogen Bonding in Solids*. Benjamin, New York (1968).
[15] M. KOBAYASHI, *J. chem. Phys.* **70**, 4797 (1979).
[16] N. NETO, M. MUNIZ-MIRANDA and E. BENEDETTI, *Macromolecules* **13**, 1302 (1980).
[17] Y. ABE and S. KRIMM, *Biopolymers* **11**, 1817 (1972).
[18] S. CALIFANO, *Vibrational States*. John Wiley, New York (1976).
[19] T. C. CHEAM, Ph.D. Thesis, University of Michigan (1982).
[20] W. H. MOORE and S. KRIMM, *Biopolymers* **15**, 2439 (1976).
[21] A. M. DWIVEDI and S. KRIMM, *Macromolecules* **15**, 177 (1982).
[22] T. SHIMANOUCHI, in *Physical Chemistry—An Advanced Treatise*, Vol. 4 (edited by H. EYRING, D. ANDERSON and W. JOST). Academic Press, New York (1970).
[23] J. L. DUNCAN, R. A. KELLY, G. D. NIVELLINI and F. TULLINI, *J. molec. Spectrosc.* **98**, 87 (1983).
[24] P. PULAY, G. FOGARASI and J. E. BOGGS, *J. chem. Phys.* **74**, 3999 (1981).
[25] H. E. HALLAM and C. M. JONES, *J. molec. Struct.* **5**, 1 (1970).
[26] L. J. BELLAMY, *Infrared Spectra of Complex Molecules*. John Wiley, New York (1975).
[27] A. I. KITAIGORODSKY, *Molecular Crystals and Molecules*. Academic Press, New York (1973).
[28] K. LONSDALE, *Acta crystallogr.* **14**, 37 (1961).
[29] D. W. J. CRUICKSHANK, *Acta crystallogr.* **9**, 1005 (1956).
[30] S. KRIMM and Y. ABE, *Proc. natn. Acad. Sci. U.S.A.* **69**, 2788 (1972).
[31] P. BOSI, G. ZERBI and E. CLEMENTI, *J. chem. Phys.* **66**, 3376 (1977).